Soft Matter

Accepted Manuscript

ROYAL SOCIETY OF CHEMISTRY

www.rsc.org/softmatter

Journal Name

ARTICLE TYPE

Cite this: DOI: 10.1039/xxxxxxxxxx

Reversible switching of liquid crystal micro-particles in a nematic liquid crystal†

Koki Imamura,[a] Hiroyuki Yoshida,*[a] and Masanori Ozaki[a]

Received Date
Accepted Date

DOI: 10.1039/xxxxxxxxxx

www.rsc.org/journalname

Liquid crystal micro-particles are functional materials possessing optical and dielectric anisotropies originating from the arrangement of rod-like molecules within the particles. Although they can be switched by an electric field, particles dispersed in isotropic hosts usually cannot return to their original state, because there is no restoration force acting on the particles. Here, we describe reversible switching of liquid crystal micro-particles by dispersing them in a nematic liquid crystal host. We fabricate square micro-particles with unidirectional molecular alignment and investigate their static and dynamic electro-optic properties as an in-plane electric field is applied. The behavior of the micro-particles is well-described by the theoretical model we construct, making this study potentially useful for the development of liquid crystal-liquid crystal particle composites with engineered properties.

1 Introduction

Liquid crystal (LC) micro-particles are attracting growing interest and have been studied in hope of developing advanced applications. LC particles are fabricated by polymerizing rod-like molecules in the liquid crystalline state; the anisotropy of the rod-like molecules is retained in the polymerized particle, thus resulting in functional particles possessing the properties of LCs. To date, LC particles with various shapes or interior molecular alignments have been fabricated through different bottom-up methods.[1–4] Moreover, their switching behavior upon applying optical[2,5–9] or electrical[10–13] stimuli have been reported. Most studies to date, however, focus on systems in which the LC particles are dispersed in an isotropic host. While LC particles can rotate with sub-ms to ms switching times in non-viscous, isotropic hosts, switching is one-way, i.e., the particles cannot be switched back to their original positions, because an isotropic host exerts no restoration force, and electrostatic torque is proportional to the square of the field (i.e., changing the polarity of a field does not reverse the switching direction). Consequently, complicated electrode structures are required to reversibly switch LC particles in an isotropic host, which is a drawback for the applications of these materials.

In this paper, we demonstrate reversible, electric-field-induced switching of anisotropic LC micro-particles in a nematic LC host. Square micro-particles with unidirectional molecular alignment are fabricated via two-photon excited direct laser writing,[14–16] dispersed in a low-molecular-weight nematic host, and driven by an electric field applied in the in-plane direction of the cell. Surface anchoring on the particles induces a twist distortion in the host LC director when there is a mismatch in the orientation direction, and generates an elastic torque which causes the particle to rotate in the direction reducing the mismatch. We had previously demonstrated spontaneous rotation of LC particles at the isotropic-nematic transition of the host LC;[14] however, the switching speed was slow (~30 s), and electric-field-induced switching had not been performed. Here we show through experiment and theory that the particles can be switched reversibly in a nematic LC host, and that the particle size and host viscosity greatly impact the response speed, with response times of a few 100 ms, which is faster than the previous study by more than a factor of 100, being achieved using a particle with side of 10 μm. This new material system may lead to new electro-optic devices such as bendable displays and e-papers.

2 Experimental

2.1 Sample Fabrication

The LC particles were fabricated from a commercial reactive mesogen (Merck, RMS03-013C) containing a photoinitiator (TCI, 2-Benzyl-2-(dimethylamino)-4'-morpholinobutyrophenone) at a concentration of 2.8 wt%. The sample showed the nematic phase below 58 °C, including room temperature. The material was injected in a 12-μm-thick glass sandwich cell coated with polyimide (JSR, AL1254), and after confirming uniaxial orientation, placed on a commercial laser scanning microscope system (Carl Zeiss, LSM 510) to perform two-photon excited direct laser writing.[17]

[a] Division of Electrical, Electronic and Information Engineering, Osaka University, 2-1 Yamadaoka, Suita, Osaka, 565-0871, Japan. E-mail: yoshida@eei.eng.osaka-u.ac.jp; Tel: +81 06 6879 7759

† Electronic Supplementary Information (ESI) available. See DOI: 10.1039/b000000x/

Because photo-polymerization occurs only in the vicinity of the laser focus, three-dimensional objects can be fabricated within a photopolymerizable resin. 100 fs pulses of an Ti:sapphire laser (Spectra Physics, Maitai) at wavelength 800 nm and a repetition rate of 80 MHz were tightly focused by an oil-immersion objective lens (×63, NA 1.4), and scanned over a square area, such that the LC orientation would be along the diagonal of the particle. Particle fabrication was performed at a laser intensity of 4.3 MW cm^{-2} and scan speed of 9 μs $μm^{-1}$, which yielded particles with a height of approximately 3 μm (confirmed from laser scanning microscopy). After microfabrication, the residual reactive mesogen was removed by placing an absorbent paper, and then mixed with a nematic LC (Merck, 5CB). Removal of the reactive mesogen was confirmed by checking the clearing point (35 °C) of the 5CB. The material was sandwiched between a 5-μm-thick sandwich cell composed of a substrate possessing interdigitated ITO electrodes with spacing of 60 μm and bare glass. The substrates were coated with the same polyimide as for the cell prepared for the fabrication of particles, and rubbed unidirectionally at an angle of 45 ° to the electrodes.

2.2 Electro-optic measurements of particles

Sample observation was performed on a polarized optical microscope (POM; Nikon, Eclipse LV100-POL) equipped with a commercial hotstage (Linkam, LTS420) set at 27 °C. A square wave electric field with frequency of 10 kHz was applied between the interdigitated electrodes and the response of the particles was recorded with a digital camera. The dynamic response of the particles was measured by inserting a band-pass filter ($\lambda = 550$ nm, $\Delta\lambda = 40$ nm) in the optical path and measuring the change in output light intensity with a photomultiplier tube. A 200-μm-core optical fiber was used in conjunction with an ×100 objective lens, corresponding to a spot diameter of approximately 2 μm.

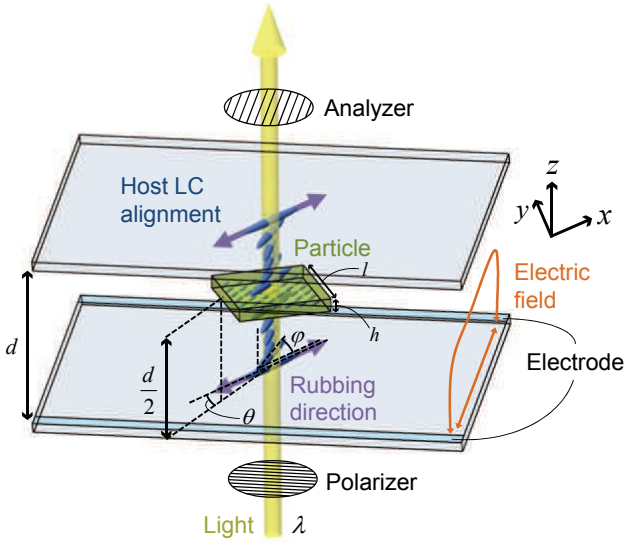

Fig. 1 Schematic of the experimental configuration for observing the electric field response of particles.

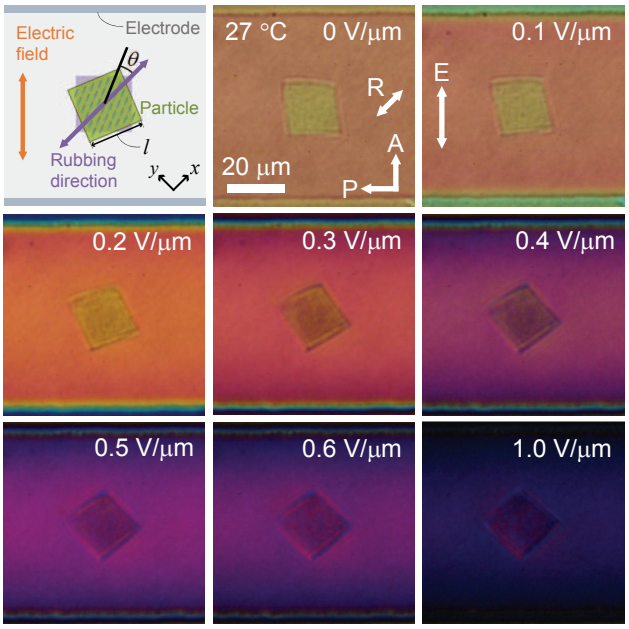

Fig. 2 Schematic (top-left) and POM images (others) of a 20 μm particle under different electric fields. The arrows labeled *P*, *A*, and *R* indicate directions of the polarizer, analyzer, and rubbing, respectively.

3 Results and discussion

3.1 Static properties of field-induced particle rotation

Figure 1 depicts the experimental configuration. Square-shaped particles with interior molecular alignment along the diagonal are floating in a sandwich cell with unidirectional LC alignment. The direction of the alignment is at 45 ° to the electrodes. Figure 2 shows the POM images of a 20 μm particle dispersed in the 5CB host. The direct laser writing process enables particles with uniform interior orientations to be fabricated, which allows us to obtain colloidal dispersions without any topological defects. The slight distortion in shape of the resultant particle is caused by the anisotropic shrinking of the liquid crystalline polymer upon photopolymerization.[18] Without an electric field, the LC particle spontaneously orients as to match their interior alignment along the rubbing direction.[14] When a square wave electric field is applied between the electrodes, the LC particle rotates so that the interior molecular alignment gradually becomes parallel to the electric field. The rotation angle is dependent on the field strength, as shown in Fig. 2. The host LC in the surrounding also changes color with the electric field, owing to a change in retardation.

Figure 3 shows the applied field dependence of the normalized orientation angle of the particles, θ/θ_{max}, where θ_{max} is the maximum displacement angle (= 45 °). The angles were measured from POM images acquired 1 min after the application of a field, to ensure that they were at equilibrium. As can be seen from Fig. 3, θ increases monotonically as the electric field becomes stronger, and reaches θ_{max} at approximately 0.7 V $μm^{-1}$ regardless of size; the 10 μm particle behaves differently from the others at low electric fields, but the behavior becomes similar for all particles above approximately 0.3 V $μm^{-1}$.

We construct a theoretical model to understand the behavior

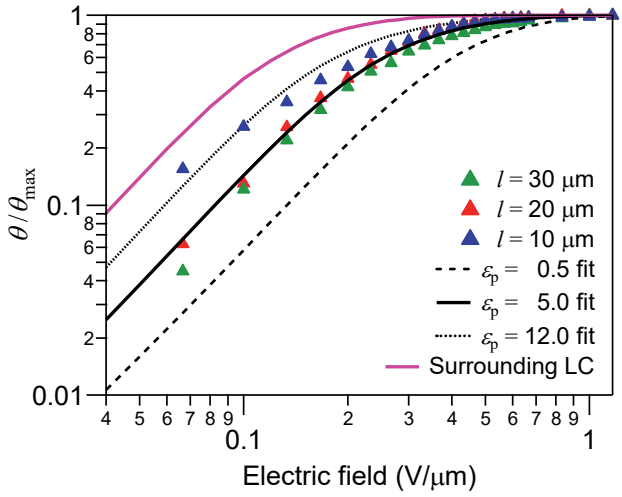

Fig. 3 The rotation angle of the particle as a function of the applied electric field. The black lines are theoretical fits employing with various ε_p values, and the pink-purple line is the theoretical rotation angle of the host LC in the middle of the cell.

in more detail. We assume that the LC particle is positioned at the middle of the cell and that no translational motion occurs. An in-plane electric field causes the LC particles to rotate owing to the electrostatic torque generated by the dielectric anisotropy of the LC particles. As the particle rotates, strong anchoring on the particle surface induces twisting of the host director between the substrate and the particle, which in turn generates an elastic torque to decrease the twist angle. Director deformation mainly comprising splay occurs in the lateral direction of the particle, but considering that the area over which such a deformation occurs is small compared to the particle size (for example, the host LC surrounding the particle appears almost uniform in Fig. 2), we ignore this contribution to simplify the analysis. The equilibrium angle upon applying a field can then be calculated as the angle that minimizes the free energy, $G(\theta)$, given by the sum of the elastic energy of the host LC and the electrostatic energy of the particle:

$$G(\theta) = 2\int_0^{\frac{d-h}{2}} \left(\frac{1}{2}K_{22}\left(\frac{d\varphi}{dz}\right)^2 - \frac{1}{4}\varepsilon_0\varepsilon_{LC}E^2\sin 2\varphi\right) dz - \frac{1}{4}\varepsilon_0\varepsilon_p E^2 h \sin 2\theta. \quad (1)$$

Here, d is the cell-gap, h is the thickness of the particle, K_{22} is the twist elastic constant of the host, $\varphi(z)$ is the twist angle distribution of the host, ε_0 is the permittivity of free space, ε_{LC} is the dielectric anisotropy of host LC, E is the applied field strength, and ε_p is the dielectric anisotropy of the particle. For a particular value of E, the combinations of $\varphi(z)$ and θ which minimize $G(\theta)$ under the boundary conditions $\varphi(0) = 0$ and $\varphi((d-h)/2) = \theta$ are determined. The black lines in Fig. 3 show theoretical fits with various ε_p values. Taking $K_{22} = 3.7$ pN[19] and $\varepsilon_{LC} = 12$[20] for 5CB, it is found that the best fit is obtained for $\varepsilon_p = 5.0$. This value is larger than the value previously reported for the photopolymerized nematic LC film (0.5[21]), but since this value is smaller than that of 5CB, we attribute this result to the host LC molecules infiltrating inside the particle. Such a phenomenon has also been reported by another group who studied the behavior of LC microspheres fabricated by microfluidics.[22]

The orientation angle of the host LC at the center of the cell (in the absence of particles) can be calculated using a similar expression as eqn (1) but ignoring the energy contribution from the particle. Its field dependence is drawn in pink-purple in Fig. 3. The results show that for a particular applied field, the rotation angle of the particle is always smaller than the rotation of the LC molecules without the particle, and that the difference between the two angles is greater at small to intermediate (the difference is greater than 50 % of the maximum difference between 0.06 and 0.38 V μm^{-1}) electric fields. Considering that this difference contributes to the director deformation in the lateral direction of the particle, and that the contribution of this deformation to the free energy is greater for smaller particles, we suspect that the deviation of the behavior of the 10 μm particle from the theoretical curve at low electric fields is due to the non-negligible contribution of the lateral deformation.

We comment on the presence of a threshold in this system. The host LC where the particle was absent showed a threshold behavior at an electric field of ~ 0.16 V μm^{-1} (Supplementary Fig. 1). As for the particles, theoretical calculations indicate that the free energy reduced by the particle rotating in the direction of field is always greater than the increase in free energy due to the induced twist distortion of the host director; i.e., the particles can rotate without a threshold (Supplementary Fig. 2). Rotation occurring at low fields, however, is very small (for example, < 0.3 ° or $\theta/\theta_{max} = 0.0067$ below 0.02 V μm^{-1}) and was not observable in experiment; rotation was clearly observed at fields higher than the threshold of the host. For practical purposes, therefore, we may say that these particles also show a threshold-like behavior at the threshold of the host LC.

3.2 Dynamic properties of particles

We now turn to the dynamic properties of the particles. Figure 4 shows typical transient response curves of a LC cell containing a 10 μm particle upon application and removal of an electric field (1.0 V μm^{-1}). The motion of the particle recorded by a video camera is shown in Supplementary Movie 1. The obtained response consists of two components: a fast component corresponding to the host LC and a slower component corresponding to the particle. It is found that for all particles sizes investigated, a double exponential function can satisfactorily describe the experimental response curves, as shown in Fig. 4. The response time of the LC particles is estimated from the time required for the slow component to rise or fall exponentially through 90% of the total process. The field dependence of the response time is evaluated and compared with that of the host LC, which is measured where the particle is absent.

Figure 5 shows the applied field dependence of the response times for particles with different sizes. It is seen that the rise time decreases monotonically with the electric field, while the decay time is almost constant; these characteristics of particles is

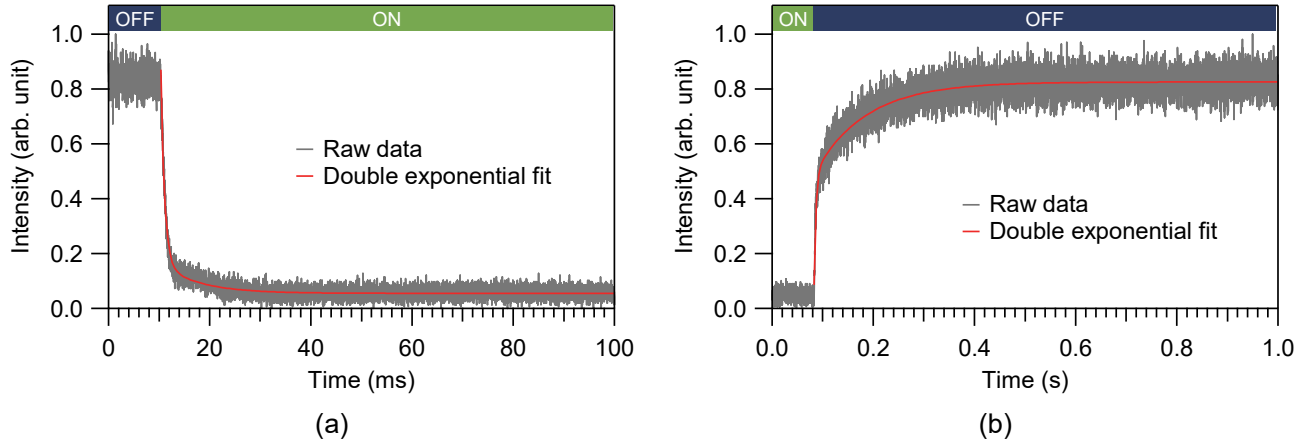

Fig. 4 Transient response of cross-polarized transmittance for a 10 μm particle upon (a) applying and (b) removing an electric field (1.0 V μm^{-1}).

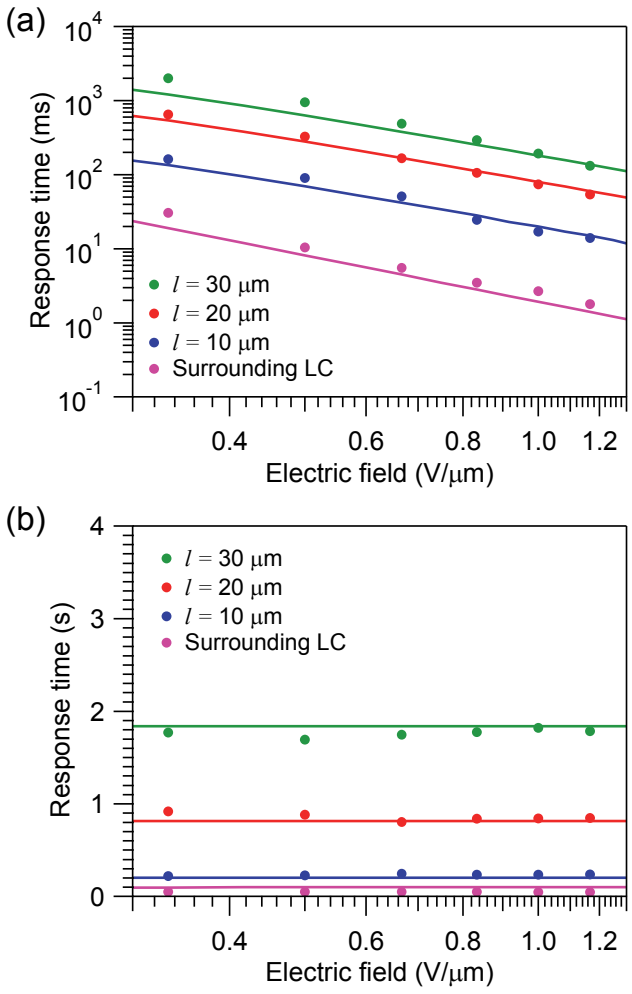

Fig. 5 Electric field dependence of response times for LC particles with different sizes upon (a) application and (b) removal of field.

similar to those of pure 5CB, which is also plotted in Fig. 5. The response becomes faster as the particle size becomes smaller for both on and off processes, and approaches the response of the host LC.

To understand this behavior theoretically, we consider a one-dimensional model similar to the one constructed for the static response, but this time assume an effective viscosity for the host to investigate the dynamics. The optical response is simulated by calculating the time-dependent director distribution of the host LC, and then calculating the cross-polarized transmittance for light with wavelength of 550 nm by Jones calculus. The Euler's equation of motion of particles is given by $I\ddot{\theta} = T - F_D$, where I is the moment of inertia, T is the torque and F_D is the viscous resistance. For the particles in this case, $I = \rho l^4 h/6$, $F_D = (2\eta_{eff} l^4/3(d-h))\dot{\theta}$ and

$$T = -2l^2 \frac{\partial}{\partial\theta}\left[\int_0^{\frac{d-h}{2}} \left(\frac{1}{2}K_{22}\left(\frac{d\varphi}{dz}\right)^2 - \frac{1}{4}\varepsilon_0\varepsilon_{LC}E^2\sin 2\varphi\right) dz\right] + \frac{1}{2}\varepsilon_0\varepsilon_p E^2 l^2 h\cos 2\theta, \quad (2)$$

where ρ is the density of particles, l is the length of a side of particles, and η_{eff} is the effective viscosity of 5CB. The best fit is obtained for η_{eff} = 32 cP, which is similar to the Miesowicz viscosities, η_{1-3}, reported in literature ($\sim 10^1 - 10^2$ cP).[23] As shown in Fig. 5, the theoretical curve can describe the response times for all three particle sizes investigated here (see also Supplementary Fig. 3). Similarly, the response of the host LC can be reproduced by employing a rotational viscosity of γ_1 = 100 cP, which is comparable to the reported value in literature ($\sim$ 80 cP).[23]

The analyses performed here have some limitations such as that it is one-dimensional, flow is not incorporated, and the response of the LC in the vicinity of particles is assumed to be much faster than that of the particle. Modeling the director field based on the Landau-de Gennes theory, considering flow effects, and simultaneously solving the motion of the host LC and the particles will possibly help improve the accuracy of the fits. Nevertheless, the model works satisfactorily for the three different sizes studied here as the same parameters could be used to describe the experimental data, and the model provides insight on the different mechanisms at play affecting the response. For example, eqn (2) can be also expressed as $T = T_{EL} + T_{ES}$, where T_{EL} (the first term in the equation) is the elastic contribution from the host LC and T_{ES} (second term) is the electrostatic contribution from the particle.

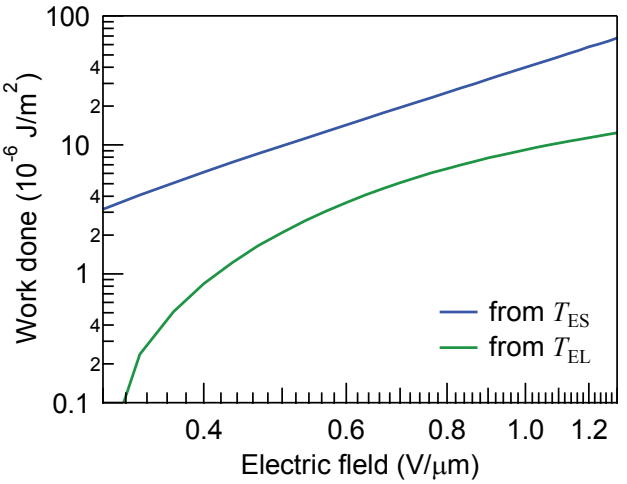

Fig. 6 Electric field dependence of work done from electrostatic (T_{ES}) and elastic (T_{EL}) contributions to the rotation of particles.

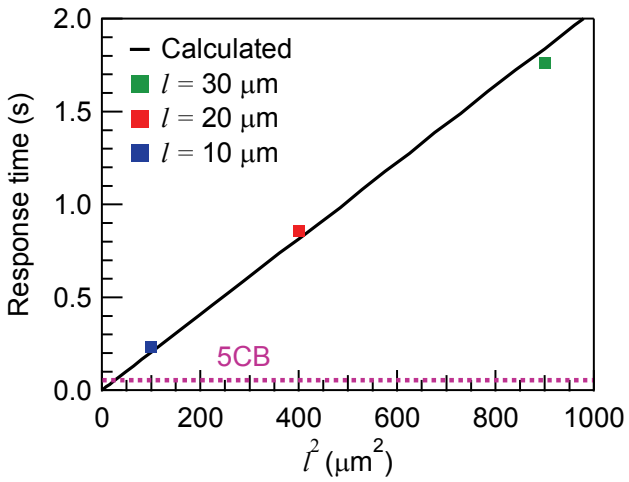

Fig. 7 Simluated size dependence of decay time of particles. Experimental mean response times of the particles and the 5CB host are shown for comparison.

By calculating the work done from T_{EL} and T_{ES}, it is found that the contribution of T_{ES} is more dominant than that of T_{EL} (Fig. 6). Increasing T_{ES} further by using particles with a larger dielectric anisotropy will likely enable particles to exhibit large rotation comparable or even surpassing the host. Also, since $I \ll 1$ in the equation of motion for micro-sized particles, we obtain $T \approx F_D$. Considering that $T \propto l^2$ and $F_D \propto l^4\dot{\theta}$, $T \approx F_D$ yields $\dot{\theta} \sim l^{-2}$, providing a physical basis for the improvement in the response speed with decreasing particle size. In fact, by simulating the free relaxation time of particles with different sizes, a near l^{-2} dependence is found as shown in Fig. 7. It is interesting to note that the theoretical model can predict the response times of particles that are only ~3 times as slow compared to 5CB, when we have assumed the response of 5CB to be much faster than the particle as to completely ignore its contribution to the change in output light intensity. This is possibly because the LC responsible for generating the elastic torque is confined between the particle and substrate, i.e., in a gap of $(d-h)/2$, instead of d. Since the response time of a nematic LC is approximately inversely proportional to the square of the cell-gap,[24] the LC between the particle and substrate can respond faster than the bulk 5CB, and hence fulfill our assumption. By exploiting the mechanisms clarified here, it may be able to fabricate particles with faster response speeds at lower fields. Such studies are planned in the future.

4 Conclusions

We demonstrated reversible electric-field switching of LC microparticles in a nematic host and described its mechanism. Downsizing of the particle size and the use of a low viscosity host enables us to achieve a relatively fast response on the order of few 10 ms. The model we constructed allows one to predict the performance of LC particles with different materials parameters. This study contributes to the understanding of LC-LC particle interactions, which is key to the future development of LC-LC particle composites with engineered properties.

Acknowledgements

This study was partly supported by JSPS KAKENHI Grant Number 15K13950 and the Photonics Advanced Research Center (PARC) at Osaka University.

References

1 Z. Yang, W. T. Huck, S. M. Clarke, A. R. Tajbakhsh and E. M. Terentjev, *Nat. mater.*, 2005, **4**, 486–490.
2 A. Fernández-Nieves, G. Cristobal, V. Garcés-Chávez, G. Spalding, K. Dholakia and D. Weitz, *Adv. Mater.*, 2005, **17**, 680–684.
3 M. Vennes, R. Zentel, M. Rössle, M. Stepputat and U. Kolb, *Adv. Mater.*, 2005, **17**, 2123–2127.
4 S. Haseloh, P. van der Schoot and R. Zentel, *Soft Matter*, 2010, **6**, 4112–4119.
5 K. Sandomirski, S. Martin, G. Maret, H. Stark and T. Gisler, *J. Phys.: Condens. Matter*, 2004, **16**, S4137.
6 M. Vennes, S. Martin, T. Gisler and R. Zentel, *Macromolecules*, 2006, **39**, 8326–8333.
7 L. Chen, Y. Li, J. Fan, H. K. Bisoyi, D. A. Weitz and Q. Li, *Adv. Opt. Mater.*, 2014, **2**, 845–848.
8 J. Fan, Y. Li, H. K. Bisoyi, R. S. Zola, D.-k. Yang, T. J. Bunning, D. A. Weitz and Q. Li, *Angew. Chem. Int. Ed.*, 2015, **54**, 2160–2164.
9 H. K. Bisoyi and Q. Li, *Acc. Chem. Res.*, 2014, **47**, 3184–3195.
10 D. R. Cairns, M. Sibulkin and G. P. Crawford, *Appl. Phys. Lett.*, 2001, **78**, 2643–2645.
11 T. Z. Kosc, K. L. Marshall, S. D. Jacobs, J. C. Lambropoulos and S. M. Faris, *Appl. Opt.*, 2002, **41**, 5362–5366.
12 S. Haseloh and R. Zentel, *Macromol. Chem. Phys.*, 2009, **210**, 1394–1401.
13 D. R. Cairns, M. S. Shafran, K. A. Sierros, W. W. Huebsch and A. J. Kessman, *Mater. Lett.*, 2010, **64**, 1133–1136.
14 H. Yoshida, G. Nakazawa, K. Tagashira and M. Ozaki, *Soft*

Matter, 2012, **8**, 11323–11327.

15 C. H. Lee, H. Yoshida, Y. Miura, A. Fujii and M. Ozaki, *Appl. Phys. Lett.*, 2008, **93**, 173509.

16 H. Yoshida, *Liq. Cryst. Today*, 2012, **21**, 3–19.

17 H. Yoshida, C. H. Lee, Y. Matsuhisa, A. Fujii and M. Ozaki, *Adv. Mater.*, 2007, **19**, 1187–1190.

18 R. Hikmet, B. Zwerver and D. Broer, *Polymer*, 1992, **33**, 89–95.

19 H. J. Coles, in *Physical Properties of Liquid Crystals: Nematics*, ed. D. A. Dunmur, A. Fukuda and G. R. Luckhurst, INSPEC: IEE, Londres (G-B), 2001, ch. 5.2.

20 R. Manohar, K. K. Pandey, A. K. Srivastava, A. K. Misra and S. P. Yadav, *J. Phys. Chem. Solids*, 2010, **71**, 1311–1315.

21 T. Kumagai, H. Yoshida and M. Ozaki, *Materials*, 2014, **7**, 1113–1121.

22 J.-H. Lee, T. Kamal, S. V. Roth, P. Zhang and S.-Y. Park, *RSC Adv.*, 2014, **4**, 40617–40625.

23 A. G. Chmielewski, *Mol. Cryst. Liq. Cryst.*, 1986, **132**, 339–352.

24 P. Yeh and C. Gu, *Optics of Liquid Crystal Displays*, Wiley, Hoboken, 2010.

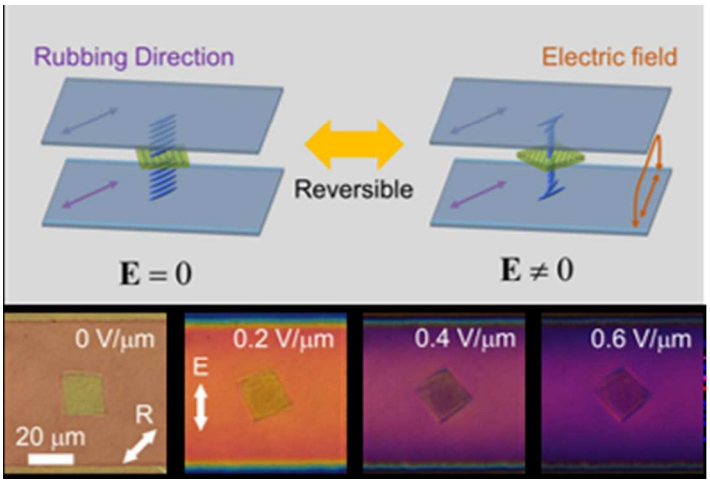

59x39mm (150 x 150 DPI)